

MINERAL PROCESSING BY SHORT CIRCUITS IN PROTOPLANETARY DISKS

COLIN P. McNALLY^{1,2,3}, ALEXANDER HUBBARD², MORDECAI-MARK MAC LOW^{2,3}, DENTON S. EBEL⁴, & PAOLA D’ALESSIO⁵

Draft version February 24, 2022

ABSTRACT

Meteoritic chondrules were formed in the early Solar System by brief heating of silicate dust to melting temperatures. Some highly refractory grains (Type B calcium-aluminum rich inclusions, CAIs) also show signs of transient heating. A similar process may occur in other protoplanetary disks, as evidenced by observations of spectra characteristic of crystalline silicates. One possible environment for this process is the turbulent magnetohydrodynamic flow thought to drive accretion in these disks. Such flows generally form thin current sheets, which are sites of magnetic reconnection and dissipate the magnetic fields amplified by a disk dynamo. We suggest that it is possible to heat precursor grains for chondrules and other high-temperature minerals in current sheets that have been concentrated by our recently described short-circuit instability. We extend our work on this process by including the effects of radiative cooling, taking into account the temperature dependence of the opacity; and by examining current sheet geometry in three-dimensional, global models of magnetorotational instability. We find that temperatures above 1600 K can be reached for favorable parameters that match the ideal global models. This mechanism could provide an efficient means of tapping the gravitational potential energy of the protoplanetary disk to heat grains strongly enough to form high-temperature minerals. The volume-filling nature of turbulent magnetic reconnection is compatible with constraints from chondrule-matrix complementarity, chondrule-chondrule complementarity, the occurrence of igneous rims, and compound chondrules. The same short-circuit mechanism may perform other high-temperature mineral processing in protoplanetary disks such as the production of crystalline silicates and CAIs.

Subject headings: instabilities — magnetic reconnection — magnetohydrodynamics — plasmas — protoplanetary disks

1. INTRODUCTION

The meteoritical record indicates that chemical and mineralogical evolution of protoplanetary disks depends on local heating processes. The ubiquity of chondrules in meteorites, along with the relation between chondrules and matrix (including chondrule-matrix elemental complementarity), appears to demand a heating mechanism that acts locally, near the assembly point of chondritic meteorites. Type B calcium-aluminum rich inclusions (CAIs), found in CV chondrites, also appear to have experienced transient heating, though under different conditions.

The basic challenge in producing chondrules is heating precursor grains with radii ~ 1 mm from below 1000 K to ~ 1800 K, and then cooling them at rates of $100\text{--}1000$ K hour^{−1}, significantly slower than expected for free radiation to a cold background (Hewins & Radomsky 1990; Lofgren & Lanier 1990; Connolly et al. 1998; Scott & Krot 2005; Ebel 2006). It further appears that heating to ~ 2000 K, followed by cooling to $1500\text{--}1800$ K at ~ 5000 K hour^{−1} is necessary to form barred textures (Connolly et al. 2006). Particularly low starting temperatures around 650 K may be required to retain the sodium and other volatile elements that

are found in some chondrules (Alexander et al. 2008), as these volatile elements will be released when the chondrules are melted. Regardless of the starting temperature, strong clustering of dust grains and rapid processing is required to avoid depletion (Alexander et al. 2008).

Examination of the chondrules and matrix in several chondritic meteorites has shown that the two constituents appear complementary in that, though the elemental makeup of each varies substantially, the bulk chemical compositions of chondrites made up of both always reflects the elemental ratios of the sun (Kornacki & Wood 1984; Bland et al. 2005; Hezel & Palme 2010). Indeed, chondrules with high variability in Fe/Si may themselves be complementary to each other, combining into parent asteroids with solar Fe/Si ratios (Ebel et al. 2008). This suggests that chondrules must have formed from local heating of matrix material. Grains from other stars (presolar grains) and insoluble organic matter found in the matrices of most primitive chondrites could not have survived the heating experienced by chondrules (Mendybaev et al. 2002; Connolly et al. 2006), establishing that the heating events were intermittent and did not process all available material. Many chondrules experienced multiple heating events, as shown by the occurrence of igneous rims (Jones 2012), and collisions with partially molten and solid droplets to produce compound chondrules (Ciesla et al. 2004). This supports the hypothesis that the chondritic meteorites are formed soon after chondrule melting, out of a dense cluster of dust grains only a fraction of which are melted. Such a scenario requires a highly localized heating source.

Type B CAIs are remelted highly refractory inclusions. They show evaporation of Mg and Si due to melting and evaporation in reheating events after condensation (Grossman et al. 2000; Richter et al. 2002; Shahar & Young 2007). Re-

cmcnally@nbi.dk, ahabbard@amnh.org, mordecai@amnh.org,
 debel@amnh.org, p.dallessio@crya.unam.mx

¹ Niels Bohr International Academy, Niels Bohr Institute, Copenhagen, Denmark

² Department of Astrophysics, American Museum of Natural History, New York, NY 10024-5192, USA

³ Department of Astronomy, Columbia University, New York, NY 10027, USA

⁴ Department of Earth and Planetary Sciences, American Museum of Natural History, New York, NY 10024-5192, USA

⁵ Centro de Radioastronomía y Astrofísica, Universidad Nacional Autónoma de México, 58089 Morelia, MICH, México

cent evidence suggests that the epochs of CAI and chondrule formation overlap (Moynier et al. 2007; Yin et al. 2009; Connelly et al. 2012).

A possible energy source for this localized heating is the magnetorotational instability (MRI), which taps the orbital energy in the disk's differential rotation to drive magnetized turbulence, transporting angular momentum outward and allowing accretion to occur (Velikhov 1959; Chandrasekhar 1960; Balbus & Hawley 1991). The MRI driven turbulence dissipates energy as heat. However, the heating occurs intermittently, not uniformly. MHD turbulence quite generally forms current sheets (Parker 1972, 1994; Cowley et al. 1997), that dissipate energy faster than the average rate. Magnetic reconnection can occur in such current sheets, enhancing their local heating rate in small regions throughout the current sheets (For a review, see Yamada et al. 2010). Hubbard et al. (2012, hereafter Paper I) showed that if the ionization depends strongly on the temperature, the dropping resistivity within the region heated by a current sheet can drive an instability effectively resulting in a short circuit, leading to strong localized heating.

One of the main diffusive processes limiting where MRI occurs in a protoplanetary disk is Ohmic resistivity, which is in turn a function of the degree of ionization of the gas. Over much of the disk, estimates suggest that the ionization near the midplane is too low for the flow to be unstable to the MRI. It is hence expected that magnetically inactive dead zones exist in these dense, cool, and almost entirely neutral regions (Gammie 1996). The secular movement of these dead zones through the disk may temporarily suppress the MRI, and thus transient heating, potentially explaining the broad range of observed chondrule ages.

The most common treatment of ionization of a protoplanetary disk includes two main components, thermal ionization of alkali metals (most importantly potassium), and nonthermal ionization from radiation (stellar ultraviolet light and x-rays, cosmic rays, and radionuclides; Armitage 2011). It has also been proposed that non-ideal MHD effects beyond Ohmic resistivity limit MRI in various regions of the disk (Blaes & Balbus 1994; Bai 2011a), and that the smallest dust grains can themselves be the dominant charge carriers in the outer disk (Bai 2011b).

This letter first presents an analysis of typical current sheet geometries in MRI driven turbulence, and then presents one-dimensional models including radiative transfer, that demonstrate that the short-circuit instability first described in Paper I can produce sufficiently high temperatures in these current sheets to implicate them in the formation of high-temperature minerals. This instability is controlled by the rapid drop in resistivity with increasing temperature that results from thermal ionization of potassium at $T > 1000$ K.

Other mechanisms for melting chondrule precursors by means of magnetic reconnection have been proposed. Sonett (1979) suggested that beams of relativistic electrons emerging from reconnection regions above or below the dense disk could heat chondrule precursors. The reconnecting magnetic fields were hypothesized to originate either from the Sun, or a disk dynamo. Along with a model for the intermittency of reconnection in a protoplanetary disk, King & Pringle (2010) proposed that magnetic reconnection regions could drive shocks strong enough to melt chondrule precursors. Formation of chondrules by ambipolar diffusion dominated reconnection was explored by Joung et al. (2004). However, that mechanism is strongly suppressed by even a small guide

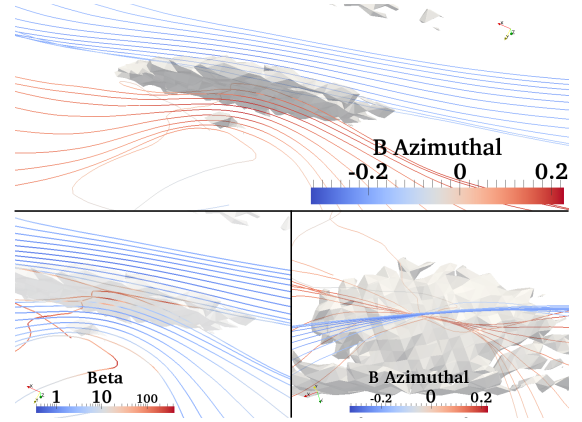


Figure 1. A typical reconnection region found in the global MRI model. The gray isosurface outlines high current density. *Upper:* Streamlines show magnetic field, colored by azimuthal component. The current sheet is bordered by oppositely directed azimuthal flux tubes. *Lower Left:* The same viewpoint as the upper panel, but the streamlines are now colored by plasma β . The value of β in the flux tubes bordering the current sheet is ~ 1 , and at least ~ 500 in the current sheet. *Lower Right:* Same quantities as the upper panel, with the viewpoint rotated to view down the short axis of the current sheet. The directions of the magnetic field in the bounding flux tubes can be seen to be nearly completely opposed. Field lines originating from points inside the current sheet where the field is weak wander significantly away from the directions of the bounding flux tubes.

field in the reconnection region (Heitsch & Zweibel 2003).

The electrical discharge mechanism of Inutsuka & Sano (2005) and Muranushi et al. (2012) may interact with the short-circuit instability, being triggered when the current sheet is sufficiently intensified.

In Section 2 we describe the bounding geometries of current sheets analyzed in a global zoom-in simulation of MRI driven turbulence. In Section 3 we demonstrate that the short-circuit instability can heat these current sheets to chondrule-forming temperatures, and that the temperature variation of opacity can lead to a self-regulated form of the instability. We discuss the results, implications, and what further work must be done to establish short circuits as a heating mechanism in protoplanetary disks in Section 4.

2. CURRENT SHEET GEOMETRIES

We used Phurbas, an adaptive, Lagrangian, meshless, MHD code (Maron et al. 2012; McNally et al. 2012), to perform a global, unstratified simulation of the MRI in a protoplanetary disk, in order to examine current sheet strength and geometry. An MRI-unstable cylindrical Keplerian shear flow with maximum radius 2.6 AU is placed in the center of a vertically periodic computational volume $40 \times 40 \times 0.4$ AU. An isothermal equation of state is used, with sound speed corresponding to a Keplerian disk with aspect ratio of 0.1, typical of protoplanetary disks. Initially, a vertical magnetic field is imposed, with a strength such that the critical MRI wavelength is one quarter of the vertical height of the volume.

Once the MRI-driven flow is reasonably saturated (as indicated by the evolution of the magnetic tilt angle), two nested, crescent-shaped, more highly refined regions that rotate with the flow are added, centered at a radius 1 AU, and extending $\sim \pi/2$ radians. These achieve resolution 1.7 and 3.4 times greater than the base flow. The Phurbas resolution parameter $\lambda = 10^{-2}$ AU in the lowest resolution region, and decreases to 2.8×10^{-3} AU in the highest resolution region. This is the region where current sheets were examined. Further details are provided in Chapter 6 of McNally (2012).

In Figure 1 we show a typical high current-density region,

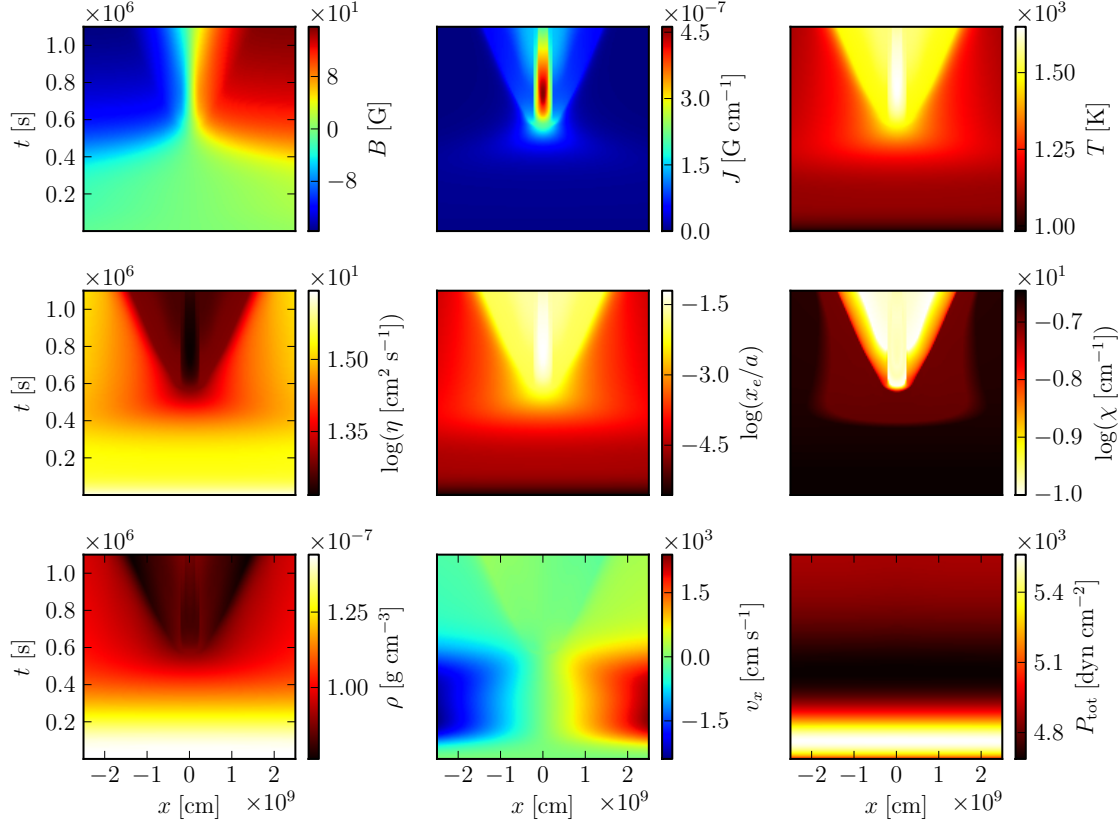


Figure 2. Heating of a current sheet bounded by $\beta = 1.5$, starting at $T_0 = 850$ K. The current sheet narrows though the short-circuit instability as the resistivity η drops. The peak temperature reached is $T \sim 1650$ K. Shown are magnetic field B , current density J , temperature T , resistivity η , potassium ionization fraction x_e/a , inverse mean photon free path χ , density ρ , velocity v_x , and total pressure P_{tot} , with respect to spatial position x and time t . The results are plotted mirrored about $x = 0$ following the boundary conditions, and only the central section of the spatial domain is shown.

which takes the form of an approximately two-dimensional current sheet sandwiched by large, nearly azimuthal flux tubes, whose magnetic field approaches the maximum field at their orbital position. The bottom panels show that there is very little perpendicular guide field passing through the center of the sheet, as the magnetic fields on the opposite sides are nearly perfectly opposed. In subsonic MHD turbulence, the expectation is that the peak currents occur at the tail of a turbulent cascade: spatially intermittent, short in duration and length scale, and randomly oriented. Peak magnetic fields generated by the MRI are, however, near equipartition, which may explain the large scale high current density regions.

We find that the current sheets retain the same general structure as the resolution is increased, while becoming thinner and more concentrated. The total, gas plus magnetic, pressure is approximately constant across these sheets, so in this locally isothermal simulation the sheets are regions of high density. From these results we conclude that a Harris-like current sheet geometry (Harris 1962) as invoked in Paper I, bounded by magnetic fields with magnetic pressure comparable to thermal pressure, is well motivated for the study of Ohmic heating in protoplanetary disks. This configuration uses a tanh profile for the magnetic field across the current sheet, and the total pressure is set constant by satisfying an adiabatic-hydrostatic condition with the temperature and density.

3. ONE DIMENSIONAL MODELS

We extended the implicit, one-dimensional, MHD code used in Paper I, which uses sixth-order finite differences on a

logarithmic grid, and the CVODE package (Hindmarsh et al. 2005) for time integration. The extensions include radiative transfer, and a full Saha-equation based treatment of the ionization of potassium (with abundance relative to hydrogen of $a = 10^{-7}$) and background nonthermal ionization. The non-thermal ionization is parameterized following equation (14) of Fromang et al. (2002), with the ionization rate $\zeta = 10^{-16} \text{ s}^{-1}$, an order of magnitude higher than the canonical value from cosmic ray ionization $\zeta = 10^{-17} \text{ s}^{-1}$. This nonthermal ionization component is used to maintain low enough resistivity to hold our artificial current sheets in place, in the absence of an active turbulent flow. This slightly increases the onset temperature of the instability and slightly weakens its growth rate, so that our model establishes a lower limit to susceptibility to the instability.

The code used in this Letter includes a radiative heating and cooling term calculated with the ray tracing scheme presented in Heinemann et al. (2006). This radiative cooling is along one dimension, as the global simulations have shown that the transverse dimensions of the current sheets are much shorter than the parallel dimensions. This allows local Ohmic heating at the center of a current sheet to heat its surroundings. With this additional physics, we have found it expedient to add a grid-scaled sixth-order hyperdiffusion to the momentum and temperature fields. Hyperdiffusions are scaled locally to the grid spacing. A logarithmic grid is specified by mapping a linear grid g which ranges from 0 to L_g to the physical coordinates x by $x(g) = f_g L_g (\exp(g/(f_g L_g)) - 1)$ where f_g is a factor which controls the grid stretching. The

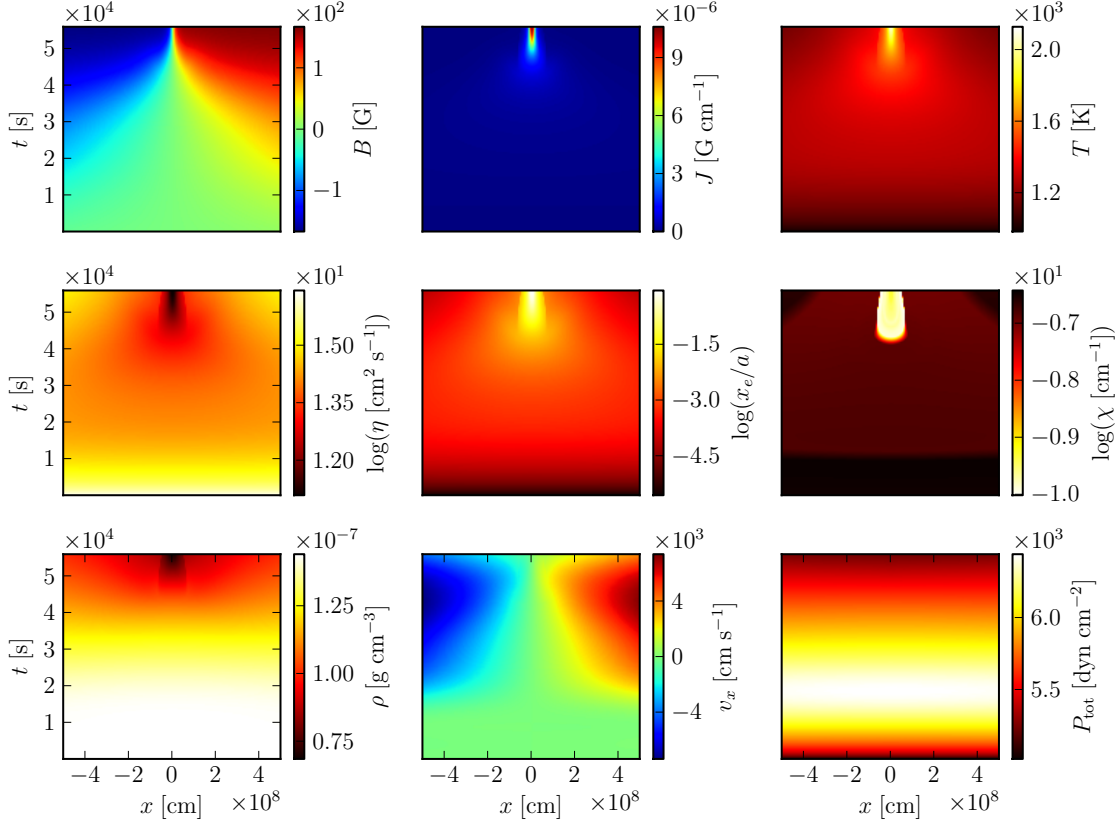


Figure 3. A thinner current sheet with width 10^{10} cm, with all other parameters identical to Figure 2, in which the potassium ionization saturates. The results are plotted mirrored about $x = 0$, and only the central section of the spatial domain is shown.

diffusion operator for a variable f is then specified directly as $\partial f / \partial t = D_g \Delta g^4 \partial^6 f / \partial g^6$, where Δg is the grid spacing increment in g , so that the diffusion scales with the grid. We also artificially smooth the variation in opacity through the addition of a finite relaxation time physically motivated by the finite vaporization time of the dust grains. Rosseland mean opacity is evolved by $\partial \kappa / \partial t = (1/t_\kappa)(\kappa_r - \kappa)$ where κ is the opacity used in radiative transfer, κ_r is the value of opacity derived from the opacity tables for the gas-dust mixture, and t_κ is a time constant. These alterations maintain the integrability of the system of equations, and we have checked that the numerical smoothing coefficients are small enough to not significantly affect the results presented here. Our initial configuration is the same as in Paper I.

The Rosseland mean opacities κ_r that we use are an updated version of the D’Alessio et al. (2001) model. Importantly, they incorporate a distribution of dust particles comprised of ice, organic, and silicate components. The sublimation temperatures of the different components are taken to be independent of the grain size, so that the opacity has a sharp transition downwards when these temperatures are reached. This model includes: graphite and “astronomical” silicates, with optical constants and fractional abundances from Weingartner & Draine (2001), and water ice with optical properties from Warren (1984). The grain size distribution is $n(r) \propto r^{-3.5}$ between $r_{min} = 0.005 \mu\text{m}$ and $r_{max} = 1 \text{ mm}$, appropriate for chondrule forming regions. The opacity is calculated using Mie theory and assuming grains are spheres. The sublimation temperatures for silicates and water ice grains are taken from Pollack et al. (1994), and for graphite, we assume

$T_{sub} = 1200 \text{ K}$. For the gas component, which is important when dust sublimates, we assume LTE. The dust-to-gas mass ratio for silicates is 4×10^{-3} , for organics, 2.5×10^{-3} , and for water ice, 4.7×10^{-3} , so in total it is 1.21×10^{-2} . Our model assumes a constant mean molecular mass $\mu = 2.32$, which is not strictly consistent with the vaporization of solids. However, we stop calculations before the dissociation of H_2 introduces a significant effect.

As discussed in Paper I, the short-circuit instability requires a strong negative dependence of the resistivity on temperature. We start our simulations with $T = T_0 = 850 \text{ K}$, where the ionization already has a rapid dependence on temperature even outside the current sheet.

In Figure 2 we show the evolution of a current sheet model with an initial ratio of thermal to magnetic pressure at the box edge of $\beta = 1.5$, background temperature $T_0 = 850 \text{ K}$, and background density $\rho_0 = 10^{-7} \text{ g cm}^{-3}$ with $B \propto \tanh(x/5 \times 10^{10} \text{ cm})$. In this configuration, the shortest wavelength for MRI, based on the length scale where the magnetic Reynolds number is unity, is on the order of $1.7 \times 10^{11} \text{ cm}$. The grid had 1000 points, $L_g = 5 \times 10^8 \text{ cm}$ and $f_g = 0.09$. Values of $D_g = 10^9 \text{ cm}^2 \text{ s}^{-1}$ in the temperature equation, and $D_g = 10^{10} \text{ cm}^2 \text{ s}^{-1}$ in the momentum equation were used. The opacity was smoothed with $t_\kappa = 2 \times 10^3 \text{ s}$. Notice in particular the small width of the narrowed current sheet. As the opacity drops, the inverse mean free path of photons χ (plotted in units of cm^{-1} in Figure 2) decreases dramatically, and an optically thin bubble is formed around the current sheet as the temperature where silicates become liquid is passed. The low opacity bubble has small internal

temperature gradients, and hence smaller resistivity gradients. As the resistivity gradient weakens, the instability shuts off. In this way the instability self-regulates. For the parameters in Figure 2, it produces heated regions with temperatures that only slightly exceed the melting temperature of the silicate grains that dominate the opacity, the largest of which produce chondrules; at this point, the instability is saturated by the increased radiative cooling. This is the most obvious configuration leading to chondrule formation.

If the current sheet is initially thinner, the heating rate becomes fast enough that the heating is not affected by the drop in opacity. Figure 3 shows the same configuration as before, except with a factor of five thinner initial current sheet $B \propto \tanh(x/10^{10} \text{ cm})$. The grid had 800 points, $L_g = 10^8 \text{ cm}$ and $f_g = 0.09$. Values of $D_g = 10^8 \text{ cm}^2 \text{ s}^{-1}$ in the temperature equation, and $D_g = 10^{10} \text{ cm}^2 \text{ s}^{-1}$ in the momentum equation were used. The opacity was smoothed with $t_\kappa = 1 \times 10^2 \text{ s}$. In this case, the short circuit instability narrows the current sheet until the potassium ionization fraction (x_e/a) reaches unity and the resistivity gradient disappears. The current sheet continues to heat as it dissipates, although we stop our calculation as it breaks down because we do not include the effects of H_2 dissociation and other changes to the effective equation of state above 2000 K.

4. DISCUSSION AND CONCLUSIONS

The models in this paper are far from a full treatment. However, they demonstrate that the short-circuit instability is a plausible candidate for chondrule formation as shown by the model in Figure 2, which starts within the range of boundary conditions for current sheets seen in our global models of protoplanetary disks, and climbs to chondrule melting temperatures within hundreds of hours. For thinner initial current sheets, the instability can reach temperatures high enough to fully ionize potassium, which is also high enough to produce barred olivine textures. This behavior is also compatible with the remelting of Type B CAIs. As the formation of the first chondrules and CAIs overlaps in time (Moynier et al. 2007; Yin et al. 2009; Connelly et al. 2012), it is plausible that the same mechanism is responsible for processing Type B CAIs and the oldest chondrules.

We have also noted that the drop in opacity associated with the destruction of organic components, at 1200 K in our opacity model, can produce a behavior similar to that in Figure 2, but at temperatures below the melting point of silicates. The temperatures produced in this type of event would be appropriate for quickly annealing amorphous silicate dust to produce crystalline silicates.

Chondrule formation by the melting of precursor grains in reconnection regions subject to the short-circuit instability of Paper I seems compatible with constraints from chondrule-matrix complementarity, chondrule-chondrule complementarity, and multiple heating listed in Section 1, as it is a local process that can occur many times to the same body of meteorite parent body precursor material.

As the MRI generates magnetic fields near equipartition with the gas thermal energy, compressive heating is a substantial contributor to the temperature. Our initial condition, as in Paper I, is chosen to be adiabatic-hydrostatic, which is the gentlest configuration we have tested. Determining the strength of the compressive heating, and its ability to meet the threshold temperature for the short-circuit instability, will require models that self-consistently form the current sheets in a large scale simulation that includes the action of temperature-

dependent resistivity. Such simulations will also allow determination of the correct physical length scale for the current sheet thickness at the onset of the instability. This length scale will strongly affect the heating and cooling times.

Furthermore, multidimensional studies of the current sheets are needed, to establish how they might break up (due to plasmod instabilities or buckling of the current sheet) and hence the size and lifetime of the heated regions, which will be important for determining the cooling rates of chondrules in this scenario. Finally, we note that the temperatures explored here have been discussed in reference only to chondrule and CAI formation. However, given more complete ionization models, other high temperature mineral processing, such as the crystallization of silicates, destruction of organics, or sublimation of ices, may occur through the same mechanism.

We thank Remo Collet for useful discussions. A.H. was partly supported by a Kalbfleisch Fellowship from the American Museum of Natural History. We also acknowledge support from the NSF through CDI grant AST08-35734, AAG grant AST10-09802, and NASA through COS grant NNX10AI42G (DSE). PD acknowledges a grant from PAPIIT-DGAPA.

REFERENCES

- Alexander, C. M. O. ., Grossman, J. N., Ebel, D. S., & Ciesla, F. J. 2008, *Science*, 320, 1617
- Armitage, P. J. 2011, *ARA&A*, 49, 195
- Bai, X.-N. 2011a, *ApJ*, 739, 50
- Bai, X.-N. 2011b, *ApJ*, 739, 51
- Balbus, S. A., & Hawley, J. F. 1991, *ApJ*, 376, 214
- Blaes, O. M., & Balbus, S. A. 1994, *ApJ*, 421, 163
- Bland, P. A., Alard, O., Benedix, G. K., Kearsley, A. T., Menzies, O. N., Watt, L. E., & Rogers, N. W. 2005, *PNAS*, 102, 13755
- Chandrasekhar, S. 1960, *PNAS*, 46, 253
- Ciesla, F. J., Lauretta, D. S., & Hood, L. L. 2004, *Meteoritics and Planetary Science*, 39, 531
- Connelly, J. N., Bizzarro, M., Krot, A. N., Nordlund, A., Wielandt, D., & A., I. M. 2012, *Science*, 338, 651
- Connolly, Jr., H. C., Desch, S. J., Ash, R. D., & Jones, R. H. 2006, in *Meteorites and the Early Solar System II*, ed. Lauretta, D. S. & McSween, H. Y. (Tucson, Arizona: University of Arizona Press), 383–397
- Connolly, Jr., H. C., Jones, B. D., & Hewins, R. H. 1998, *Geochim. Cosmochim. Acta*, 62, 2725
- Cowley, S. C., Longcope, D. W., & Sudan, R. N. 1997, *Phys. Rep.*, 283, 227
- D'Alessio, P., Calvet, N., & Hartmann, L. 2001, *ApJ*, 553, 321
- Ebel, D. S. 2006, in *Meteorites and the Early Solar System II*, ed. D. S. Lauretta & H. Y. McSween (Tucson, Arizona: University of Arizona Press), 253–277
- Ebel, D. S., Weisberg, M. K., Hertz, J., & Campbell, A. J. 2008, *Meteoritics and Planetary Science*, 43, 1725
- Fromang, S., Terquem, C., & Balbus, S. A. 2002, *MNRAS*, 329, 18
- Gammie, C. F. 1996, *ApJ*, 457, 355
- Grossman, L., Ebel, D. S., Simon, S. B., Davis, A. M., Richter, F. M., & Parsad, N. M. 2000, *Geochim. Cosmochim. Acta*, 64, 2879
- Harris, E. G. 1962, *Il Nuovo Cimento*, 23, 115
- Heinemann, T., Dobler, W., Nordlund, A., & Brandenburg, A. 2006, *A&A*, 448, 731
- Heitsch, F., & Zweibel, E. G. 2003, *ApJ*, 590, 291
- Hewins, R. H., & Radomsky, P. M. 1990, *Meteoritics*, 25, 309
- Hezel, D. C., & Palme, H. 2010, *Earth and Planetary Science Letters*, 294, 85
- Hindmarsh, A. C., Brown, P. N., Grant, K. E., Lee, S. L., Serban, R., Shumaker, D. E., & Woodward, C. S. 2005, *ACM Trans. Math. Softw.*, 31, 363
- Hubbard, A., McNally, C. P., & Mac Low, M.-M. 2012, *ApJ*, 761, 58
- Inutsuka, S.-i., & Sano, T. 2005, *ApJ*, 628, L155
- Jones, R. H. 2012, *Meteoritics and Planetary Science*, 47, 1176
- Joung, M. K. R., Mac Low, M.-M., & Ebel, D. S. 2004, *ApJ*, 606, 532
- King, A. R., & Pringle, J. E. 2010, *MNRAS*, 404, 1903

- Kornacki, A. S., & Wood, J. A. 1984, *Geochim. Cosmochim. Acta*, 48, 1663
- Lofgren, G., & Lanier, A. B. 1990, *Geochim. Cosmochim. Acta*, 54, 3537
- Maron, J. L., McNally, C. P., & Mac Low, M.-M. 2012, *ApJS*, 200, 6
- McNally, C. P. 2012, Dissertation, Columbia University in the City of New York
- McNally, C. P., Maron, J. L., & Mac Low, M.-M. 2012, *ApJS*, 200, 7
- Mendybaev, R. A., Beckett, J. R., Grossman, L., Stolper, E., Cooper, R. F., & Bradley, J. P. 2002, *Geochim. Cosmochim. Acta*, 66, 661
- Moynier, F., Yin, Q.-z., & Jacobsen, B. 2007, *ApJ*, 671, L181
- Muranushi, T., Okuzumi, S., & Inutsuka, S.-i. 2012, *ApJ*, 760, 56
- Parker, E. N. 1972, *ApJ*, 174, 499
- Parker, E. N. 1994, Spontaneous current sheets in magnetic fields : with applications to stellar x-rays. International Series in Astronomy and Astrophysics, Vol. 1. New York : Oxford University Press, 1994., 1
- Pollack, J. B., Hollenbach, D., Beckwith, S., Simonelli, D. P., Roush, T., & Fong, W. 1994, *ApJ*, 421, 615
- Richter, F. M., Davis, A. M., Ebel, D. S., & Hashimoto, A. 2002, *Geochim. Cosmochim. Acta*, 66, 521
- Scott, E. R. D., & Krot, A. N. 2005, in Astronomical Society of the Pacific Conference Series, Vol. 341, Chondrites and the Protoplanetary Disk, ed. A. N. Krot, E. R. D. Scott, & B. Reipurth, 15
- Shahar, A., & Young, E. D. 2007, *Earth and Planetary Science Letters*, 257, 497
- Sonett, C. P. 1979, *Geophys. Res. Lett.*, 6, 677
- Velikhov, E. P. 1959, *J. Exptl. Theoret. Phys.*, 36, 13981404
- Warren, S. G. 1984, *Appl. Opt.*, 23, 1206
- Weingartner, J. C., & Draine, B. T. 2001, *ApJ*, 548, 296
- Yamada, M., Kulsrud, R., & Ji, H. 2010, *Rev. Mod. Phys.*, 82, 603
- Yin, Q.-Z., Yamashita, K., Yamakawa, A., Tanaka, R., Jacobsen, B., Ebel, D., Hutcheon, I. D., & Nakamura, E. 2009, in Lunar and Planetary Inst. Technical Report, Vol. 40, Lunar and Planetary Institute Science Conference Abstracts, 2006